Automatica 123 (2021) 109302

Contents lists available at ScienceDirect

Automatica

journal homepage: www.elsevier.com/locate/automatica

Brief paper

A nonlinear control strategy for robust tracking under exogenous vibrations for in-line nano-metrology☆

Saverio Messineo

Department of Electronic Systems, NTNU, O.S. Bragstads Plass 2B, 7034 Trondheim, Norway

ARTICLE INFO

Article history:
Received 27 October 2019
Received in revised form 29 July 2020
Accepted 16 September 2020
Available online 19 October 2020

Keywords:
Robust tracking
Exogenous vibrations
Nonlinear control
Learning observer
Error feedback

ABSTRACT

This paper proposes a novel, observer-based, nonlinear control strategy aimed at facilitating the pursuit of nanomechanical measurements within the noisy environments of industrial production lines. The investigation makes use of a laboratory-prototype emulating an architecture composed by a sample to be analyzed, and by a metrology platform whose task is to carry out in-line measurements, while the whole system is being affected by exogenous vibrations. The control objective is to lock the distance between the metrology platform and the sample, thereby allowing the pursuit of the measurement task. The proposed solution achieves robustness with respect to unknown plant parameters and exogenous disturbances by means of a combination of high-frequency and high-gain tools, and by relying on a novel "learning observer". The proposed design is formally analyzed, and then experimentally validated by providing a comparative study with a PID-based control-strategy. The experimental results indicate, overall, a favorable performance of the proposed control algorithm over the PID counterpart.

1. Introduction

Keeping track of nanomechanical properties such as adhesion, hardness or roughness is of major significance for quality-control purposes, as the latter are at the root of phenomena such as energy loss, reduced tool-lifetime and loss of accuracy (Leach, 2009). However, as opposed to the "protected" vibration-free scientific environments, where such measurements are typically carried out by means – for instance – of atomic force microscopes (Eaton & West, 2010), industrial production lines pose the additional challenge of being inherently affected by disturbances (in the form of detrimental vibrations) due to the presence of several machines and personnel (Subrahmanyan, 1999). Because of this further complication, instruments such as the atomic force microscope, for the purpose of being used in-line, need to be equipped with a component devoted to the pursuit of the disturbance rejection task.

Up to the author's knowledge, the problem under consideration has only been addressed in Ito et al. (2015) and Thier et al. (2016), from a mechatronics standpoint. In line with such philosophy, in the cited works a major emphasis was placed – rather than on the control design – on the study, design and physical realization of ad hoc mechanical structures aimed at decoupling the environmental disturbances from the measurement instrumentation. The proposed strategies were then completed by a control system which was derived within the frequency domain (hence, by not leaving any room for a possible nonlinear design) and that was based on the prior identification of the system to be controlled — hence producing an inherently non-robust control design. On the other hand, and to the best of the author's knowledge, this problem has *never* been addressed from a control-system standpoint. Hence, the main contribution of this paper is to fill this gap by proposing – in a dual fashion with respect to the works in Ito et al. (2015) and Thier et al. (2016) – a novel nonlinear and robust control system design, that solves the problem under consideration. The focus is on control-design, and no mechanical design is considered.

For such purpose, a pre-existing laboratory-prototype is employed for the task of emulating a system composed by a sample to be analyzed, and by a metrology platform (equipped with an actuation system to control its motion) aimed at performing nanomechanical measurements, in the presence of detrimental vibrations. Then, within this experimental framework, a novel control system design is proposed with the aim of enforcing a desired constant distance between the sample and the metrology platform, so as to facilitate the measurement task in the presence of exogenous vibrations. As opposed to the works in Ito et al. (2015) and Thier et al. (2016), the proposed solution will be robust with respect to the model parameters (in that, their

☆ This work was partially supported by the "aim4np" (Norway) project, within the EU FP7 scheme. The material in this paper was not presented at any conference. This paper was recommended for publication in revised form by Associate Editor Angelo Alessandri under the direction of Editor Thomas Parisini.

E-mail address: saverio.messineo@ieee.org.

https://doi.org/10.1016/j.automatica.2020.109302

prior knowledge shall not be assumed, and so that, the proposed strategy shall function for a set of model parameters as large as desired), and it will do so by exploiting the possibilities offered by the theory of nonlinear control in the form of high-frequency and high-gain tools. In addition, aided by a dedicated sensor measuring the distance between the metrology platform and the sample, the proposed control design shall make use of a novel "learning observer" devoted to the reconstruction of the missing velocity information. The observer is derived by exploiting techniques within the area of the second-order sliding mode control and in particular, by a re-visitation of the work in Xian et al. (2004), and will display the capability of achieving perfect asymptotic velocity-reconstruction in spite of unknown model parameters, but without having to resort to parameter-reconstruction (hence yielding a *non*-model based estimation). Being such the case, then the proposed observer naturally provides an improvement over the on-line differentiators (known as "High-gain observers") presented in the seminal work in Esfandiari and Khalil (1992), as the latter could only yield an approximated reconstruction (however, up to a desired level of precision) of the derivative information. This constitutes the second contribution of the paper. Then, on the basis of the reconstructed quantity, the control design is pursued in a certainty-equivalence fashion, and a separation-principle will be formally shown to hold for the proposed nonlinear control architecture, providing the third contribution of the paper.

The paper is organized as follows: Section 2 describes the experimental setting and provides a mathematical model for control. In Section 3, the control problem is formulated. Section 4 presents the observer strategy, followed by the control system design in Section 5. Experimental results are presented and discussed in Section 6, followed by concluding remarks.

2. Modeling

In this section, first a description of the experimental setting is given, then, a mathematical model for control is derived.

2.1. Experimental setting

With reference to Fig. 1 depicting the experimental scale-model, the sample is emulated by a mass attached to the bottom moving-coil loudspeaker. The latter is employed as a sample-shaker, which, by exploiting the Lorentz force (denoted by F_l in the sketch of the laboratory prototype in Fig. 1), shall be actively driven in order to produce vibrations. Similarly, the metrology platform is emulated by a second mass attached to the top moving-coil loudspeaker. By employing an eddy current sensor mounted between the two masses, and, as such, measuring their relative distance, the role of the top loudspeaker is providing the actuation force (denoted by F in the sketch of the laboratory prototype in Fig. 1) necessary to enforce a motion on the metrology-platform mass (henceforth referred to as "metrology platform"). Both sample and metrology platform are additionally affected by the laboratory environmental vibrations. On the contrary, because the mass of the top base (formed by the top loudspeaker stator and a wooden structure) is far greater than the one of the subsystem composed by the top loudspeaker and the metrology platform, then the reactive forces directed from the latter towards the top base are neglected.

The real-time control system is implemented on a dSpace DS1103 controller board hosted by a PC. The sensor signals are connected to the dSpace board by means of 16-bit ADC converters, whereas 16-bit DAC converters, along with power amplifiers are used for actuation.

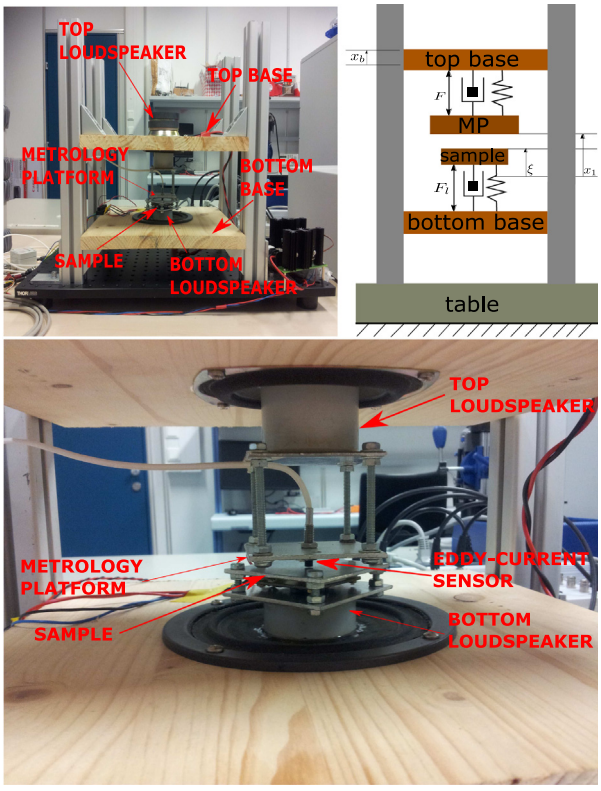

Fig. 1. Laboratory-prototype (top left); sketch of the laboratory-prototype (top right); laboratory-prototype zoomed view (bottom).

2.2. Coordinates definition and mathematical modeling

In Fig. 1 (top right) a sketch of the experimental setup is shown along with a definition of references and coordinates. Consider all coordinates positive when pointing upwards, and regard the lab where the actual experiments are carried out (devoid of any vibration arising from the ground) as an inertial frame. Then, the motion $x_1(t)$ of the metrology platform is defined with respect to the inertial frame (henceforth denoted by Σ) whose origin coincides with the metrology platform rest position relative to the lab, when the gravity force contribution is taken into account, but in absence of both Lorentz force exerted by the actuator and vibrations arising from the ground. The sample motion $\xi(t)$ is defined with respect to the inertial frame Σ as well: this is done so that the quantity $x_1(t)-\xi(t)$ corresponds to the distance between the metrology platform and the sample; hence, $x_1(t) = \xi(t)$ if and only if the sample and the metrology platform are in contact. The motion $x_b(t)$ of the top base is defined with respect to an inertial frame whose origin, $x_b = 0$, coincides with the rest position of the base-structure with respect to the lab, when no external vibrations arise from the ground.

With reference to Egeland and Gravdahl (2003, pag. 109-110), and by accounting for the vibrations affecting the base, the dynamics of the system composed by the top loudspeaker and the metrology platform, reads as

$$L\frac{di}{dt} = -Ri - K_e(\dot{x}_1 - \dot{x}_b) + v \tag{1}$$

$$m\ddot{x}_1 = -k_0(x_1 - x_b) - d_0(\dot{x}_1 - \dot{x}_b) + F \tag{2}$$

with (1) describing the electrical dynamics, and (2) the mechanical ones. In system (1)–(2), L stands for the circuit inductance, R the resistance, $K_e(\dot{x}_1 - \dot{x}_b)$ the induced voltage, v the voltage control input, m the mass, k_0 the stiffness, d_0 the damping,

$F = K_e i$ the Lorentz force and K_e the force factor. As a result of the specifically adopted coordinate-system, it is seen that the contribution of the acceleration of gravity g does not explicitly enter the dynamics in (2). For control-design purposes, a choice is made to neglect the fast electrical dynamics in (1); hence, by assuming $L\frac{di}{dt} = 0$, one obtains $i = \frac{v}{R} - \frac{K_e}{R}(\dot{x}_1 - \dot{x}_b)$. From the latter and from Eq. (2), by defining $\bar{k} = \frac{k_0}{m} > 0$, $d = \frac{1}{m}(d_0 + \frac{k_e^2}{R}) > 0$, $b = \frac{k_e}{mR} > 0$, and $x_2 = \dot{x}_1$, the system to be controlled can be given the following form

$$\dot{x}_1 = x_2$$
$$\dot{x}_2 = -\bar{k}(x_1 - x_b) - d(x_2 - \dot{x}_b) + bv \tag{3}$$

where $\bar{k}$, d and b are positive parameters by construction.

3. Control problem

The problem addressed herein consists in seeking a robust control strategy capable of locking the distance between the metrology platform and the sample to a constant prescribed value $c > 0$, in spite of the disturbances affecting the system. In view of this, by defining the regulation error as $e_1 = x_1 - \xi(t) - c$, by denoting its derivative by $e_2 = \dot{e}_1$, by collecting the "disturbances" into $\zeta(t) = -\bar{k}(\xi(t) + c - x_b(t)) - d(\dot{\xi}(t) - \dot{x}_b(t)) - \ddot{\xi}(t)$ (which is a uniformly bounded quantity by construction), and by applying the *preliminary control action* $v = -\bar{k}_1 e_1 + u$, with $\bar{k}_1 > 0$, then system (3) can be written in error coordinates as

$$\dot{e}_1 = e_2$$
$$\dot{e}_2 = -ke_1 - de_2 + \zeta(t) + bu \tag{4}$$

where $k = \bar{k} + b\bar{k}_1$ in (4) is a positive quantity by construction. System (4) shall be regarded as the plant to be controlled, with u playing the role of the control input. The sought control solution will be derived under a rather standard assumption, which is reported below:

Assumption 3.1. The plant parameters in (4) are such that $k \in [k_m, k_M]$, $d \in [d_m, d_M]$ and $b \in [b_m, b_M]$, with k_m, d_m and b_m positive.

The control task can hence be formally cast as follows: Given system (4) and given compact sets as in Assumption 3.1, find a robust control law such that the closed loop-trajectories are bounded, and such that, for any desired $c > 0$ and $\epsilon > 0$, there exists a time $t^* > 0$ such that, for any $t \geq t^*$, the regulation error satisfies $|e_1| \leq \epsilon$.

It is additionally noted that the regulation error e_1 is a measured quantity, whereas e_2 is not. Hence, an observer that estimates e_2 will be designed, as described next.

4. Learning observer

The proposed observer is defined as follows:

Definition 4.1. By denoting by $\hat{e}_1$ and $\hat{e}_2$, the estimates of the regulation error e_1, and, respectively, of the regulation error derivative e_2 in system (4), the observer dynamics is chosen as:

$$\dot{\hat{e}}_1 = \gamma_1 \tilde{e}_1 + \hat{e}_2$$
$$\dot{\hat{e}}_2 = \gamma_2 \tilde{e}_1 + \frac{\tilde{e}_1 p^2}{|\tilde{e}_1|\, p + \delta(t)} \tag{5}$$

with $\tilde{e}_1 = e_1 - \hat{e}_1$ representing the estimation error in reconstructing e_1, where γ_1, γ_2 and p are positive gains, and where $\delta(t)$ is selected as a positive function for any $t \geq 0$ which must satisfy: $\delta(t) \to 0$ as $t \to \infty$, while having $\int_0^t \delta(\tau)d\tau$ as a uniformly bounded function of time.

Furthermore, by defining $\tilde{e}_2 = e_2 - \hat{e}_2$ (denoting the estimation error in reconstructing e_2), the dynamics in (5) can be given the following alternative characterization to be used in subsequent derivations:

$$\dot{\tilde{e}}_1 = -\gamma_1 \tilde{e}_1 + \tilde{e}_2$$
$$\dot{\tilde{e}}_2 = -\gamma_2 \tilde{e}_1 - \frac{\tilde{e}_1 p^2}{|\tilde{e}_1|\, p + \delta(t)} + \dot{e}_2. \tag{6}$$

4.1. Observer convergence analysis

In order to analyze the convergence properties of the proposed observer, the following property shall be used

Property 4.1. *Define* $\mathbf{e} = (e_1, e_2)^T$ *and* $\hat{\mathbf{e}} = (\hat{e}_1, \hat{e}_2)^T$, *then there exists a family* $\mathcal{C}$ *of controllers, such that:*

1. *whenever* $u = u^*(t, \mathbf{e}, \hat{\mathbf{e}}) \in \mathcal{C}$ *in* (4), *then the trajectories* (4)–(5) *are globally well-defined for any* $t \geq 0$
2. *whenever* $u = u^*(t, \mathbf{e}, \hat{\mathbf{e}}) \in \mathcal{C}$, *then the trajectories* $e_1(t)$, $e_2(t)$ *(and hence* $\dot{e}_2(t)$*), within the closed-loop system* (4)–(5), *are globally bounded*
3. *whenever* $u = u^*(t, \mathbf{e}, \hat{\mathbf{e}}) \in \mathcal{C}$, *then, for any given compact set* $\mathcal{K} \subset \mathbb{R}^2$, *any given set in Assumption 3.1, and any given* $\zeta(t)$ *in* (4), *there exists a number* $e_\infty > 0$, *independent of* $\hat{\mathbf{e}}$, p, γ_1 *and* γ_2 *in* (5), *such that* $|e_2(t)| \leq e_\infty$ *and* $|\dot{e}_2(t)| \leq e_\infty$, *for any* $t \geq 0$, *for any initial condition* $\mathbf{e}(0) \in \mathcal{K}$, *and* $\hat{\mathbf{e}}(0) \in \mathbb{R}^2$, *within the closed-loop system* (4)–(5).

Proof. The proof is deferred to the Appendix. □

In view of Property 4.1, the following can be derived:

Property 4.2. *Select* $u = u^*(t, \mathbf{e}, \hat{\mathbf{e}})$ *in* (4); *then the trajectories of system* (5) *and the ones of system* (6) *are globally bounded. Moreover,* $\dot{\tilde{e}}_1$ *is uniformly continuous.*

Proof. Since $u = u^*(t, \mathbf{e}, \hat{\mathbf{e}})$ in (4), then Property 4.1 holds. Then define the "filtered regulation error" (Xian et al., 2004) $r(t)$ as $r = \dot{\tilde{e}}_1 + \alpha \tilde{e}_1$, where $\alpha > 0$ determines the bandwidth of the resulting first order system. In addition define $\gamma_1 = k_1 + \alpha$ and $\gamma_2 = k_1 \alpha$, with $k_1 > 0$. Then, from (6), the following dynamics can be derived:

$$\dot{\tilde{e}}_1 = -\alpha \tilde{e}_1 + r$$
$$\dot{r} = -k_1 r - \frac{\tilde{e}_1 p^2}{|\tilde{e}_1|\, p + \delta(t)} + \dot{e}_2. \tag{7}$$

Since $\delta(t) > 0$, then $\frac{|\tilde{e}_1| p^2}{|\tilde{e}_1| p + \delta(t)} \leq p$, and since $\dot{e}_2 \in \mathcal{L}_\infty$, system (7) can be regarded as an asymptotically stable linear system forced by a uniformly bounded disturbance given by the sum of the second and third terms on the right-hand side of the second equation in (7). As a result, the following properties can be inferred: $\tilde{e}_1 \in \mathcal{L}_\infty$, $r \in \mathcal{L}_\infty$, which in turn implies that $\dot{\tilde{e}}_1 \in \mathcal{L}_\infty$ and $\dot{r} \in \mathcal{L}_\infty$; moreover, since $\dot{r} = \ddot{\tilde{e}}_1 + \alpha \dot{\tilde{e}}_1$, then $\ddot{\tilde{e}}_1 \in \mathcal{L}_\infty$ as well. In addition, since $e_1 \in \mathcal{L}_\infty$ and $\tilde{e}_1 \in \mathcal{L}_\infty$, then $\hat{e}_1 \in \mathcal{L}_\infty$, too. From the first equation in system (6), by using $\tilde{e}_2 = e_2 - \hat{e}_2$, it is seen that boundedness of both $\tilde{e}_1$ and $\dot{\tilde{e}}_1$ along with the fact that $e_2 \in \mathcal{L}_\infty$, implies that $\hat{e}_2 \in \mathcal{L}_\infty$ and hence that $\tilde{e}_2 \in \mathcal{L}_\infty$, too. Finally, boundedness of $\ddot{\tilde{e}}_1$, implies that $\dot{\tilde{e}}_1$ is uniformly continuous. □

To proceed with the analysis, the following two theorems will be exploited (both of them being a straightforward application of Barbalat's lemma (Khalil, 2002, p. 323)):

Theorem 1. *If* $\lim_{t\to\infty} \int_0^t \dot{\tilde{e}}_1(\tau)d\tau$ *exists and is finite, since* $\dot{\tilde{e}}_1$ *is uniformly continuous, then* $\lim_{t\to\infty} \dot{\tilde{e}}_1 = 0$.

Theorem 2. *If $\tilde{e}_1 \in \mathcal{L}_2$, since $\tilde{e}_1 \in \mathcal{L}_\infty$ and $\dot{\tilde{e}}_1 \in \mathcal{L}_\infty$, then* $\lim_{t\to\infty} \tilde{e}_1 = 0$.

In the following, convergence to zero of both $\dot{\tilde{e}}_1$ and $\tilde{e}_1$ will be shown to hold, by proving that the conditions of Theorems 1 and 2 are fulfilled. In this way, from the first equation in (6), convergence of $\tilde{e}_2$ to zero will follow as well. To this aim, the following property will be used:

Property 4.3. *Consider system (7), and in particular, the gains p and α within it. Then, whenever $u = u^*(t, \mathbf{e}, \hat{\mathbf{e}}) \in \mathcal{C}$ in (4), it follows that, for any given compact set $\mathcal{K} \subset \mathbb{R}^2$, any given set in Assumption 3.1, and any given $\zeta(t)$ in (4), there exist $p^* > 0$ large enough and $\alpha^* > 0$ large enough, and a time $t_1 > 0$, such that:*

$$|\dot{e}_2| + \frac{1}{\alpha}|\ddot{e}_2| \le p \quad \text{for } p \ge p^*,\ \alpha \ge \alpha^*,\ t \ge t_1 \tag{8}$$

for any $\mathbf{e}(0) \in \mathcal{K}$, $\hat{\mathbf{e}}(0) \in \mathbb{R}^2$, within system (4)–(5).

Proof. The proof is deferred to the Appendix. □

The following lemma can now be proven:

Lemma 3. *Define $J = \int_0^t r\left(\dot{e}_2 - \frac{\tilde{e}_1 p^2}{|\tilde{e}_1|p+\delta(\tau)}\right)d\tau$. Then, whenever $u = u^*(t, \mathbf{e}, \hat{\mathbf{e}}) \in \mathcal{C}$ in (4), it follows that, for any given compact set $\mathcal{K} \subset \mathbb{R}^2$, any given set in Assumption 3.1, and any given $\zeta(t)$ in (4), there exist $p^* > 0$, $\alpha^* > 0$, and a finite number $J_\infty > 0$ such that:*

$$J \le J_\infty \quad \text{for } p \ge p^*,\ \alpha \ge \alpha^* \tag{9}$$

for any $\mathbf{e}(0) \in \mathcal{K}$, $\hat{\mathbf{e}}(0) \in \mathbb{R}^2$, within the closed-loop system (4)–(5), with p and α in (7).

Proof. Fix arbitrarily: the compact set $\mathcal{K} \subset \mathbb{R}^2$, the sets in Assumption 3.1, and $\zeta(t) \in \mathcal{L}_\infty$ in (4). Then consider the closed-loop system (4)–(5), with $\mathbf{e}(0) \in \mathcal{K}$ and $u = u^*(t, \mathbf{e}, \hat{\mathbf{e}}) \in \mathcal{C}$ in (4). A straightforward application of the arguments in Xian et al. (2004, Lemma 1) yields: $J \le -\int_0^t \alpha|\tilde{e}_1|\frac{|\tilde{e}_1|p^2}{|\tilde{e}_1|p+\delta(\tau)}d\tau + \int_0^t \alpha|\tilde{e}_1|\left(|\dot{e}_2| + \frac{1}{\alpha}|\ddot{e}_2|\right)d\tau + \tilde{e}_1\dot{e}_2|_0^t + 2p|\tilde{e}_1(0)|$. By then using Property 4.3, it follows that there exist $p^* > 0$, $\alpha^* > 0$ and a time $t_1 > 0$ such that, for any $p \ge p^*$, $\alpha \ge \alpha^*$ and $t \ge t_1$, then: $\int_{t_1}^t \alpha|\tilde{e}_1|\left(|\dot{e}_2| + \frac{1}{\alpha}|\ddot{e}_2|\right)d\tau \le \int_{t_1}^t \alpha|\tilde{e}_1|pd\tau$. As a result, by selecting once and for all p and α such that $p \ge p^*$ and $\alpha \ge \alpha^*$, and by noticing that $|\tilde{e}_1|\left(-\frac{|\tilde{e}_1|p^2}{|\tilde{e}_1|p+\delta(\tau)} + p\right) = \frac{|\tilde{e}_1|p\delta(t)}{|\tilde{e}_1|p+\delta(t)} \le \delta(t)$, it is possible to write $J \le \int_0^{t_1} \alpha|\tilde{e}_1|\left(-\frac{|\tilde{e}_1|p^2}{|\tilde{e}_1|p+\delta(\tau)} + |\dot{e}_2| + \frac{1}{\alpha}|\ddot{e}_2|\right)d\tau + \tilde{e}_1\dot{e}_2|_0^t + \alpha\int_{t_1}^t \delta(\tau)d\tau + 2p|\tilde{e}_1(0)|$. Since t_1 is finite, since no quantity on the right-hand side of the previous inequality has finite escape time, since $\tilde{e}_1$, $\dot{e}_2$ and $\alpha\int_{t_1}^t \delta(\tau)d\tau$ are uniformly bounded, then there exists a finite number $J_\infty > 0$ such that $J \le J_\infty$, as required. □

The following theorem shows that the observer (5) asymptotically learns (i.e., estimates) the state e_2.

Theorem 4. *Whenever $u = u^*(t, \mathbf{e}, \hat{\mathbf{e}}) \in \mathcal{C}$ in (4), then, for any given compact set $\mathcal{K} \subset \mathbb{R}^2$, any given set in Assumption 3.1, and any given $\zeta(t)$ in (4), there exist $p^* > 0$, $\gamma_1^* > 0$ and $\gamma_2^* > 0$, such that, for any $p \ge p^*$, $\gamma_1 \ge \gamma_1^*$ and $\gamma_2 \ge \gamma_2^*$ within the observer dynamics in (5), and for any $\mathbf{e}(0) \in \mathcal{K}$, and $\hat{\mathbf{e}}(0) \in \mathbb{R}^2$ within the closed-loop system (4)–(5), the following holds:* $\lim_{t\to\infty} \tilde{e}_2 = 0$.

Proof. Fix arbitrarily: the compact set $\mathcal{K} \subset \mathbb{R}^2$, the sets in Assumption 3.1, and $\zeta(t) \in \mathcal{L}_\infty$ in (4). Then, consider the closed-loop interconnection (4)–(5), whose trajectories satisfy $\mathbf{e}(0) \in \mathcal{K}$, with $u = u^*(t, \mathbf{e}, \hat{\mathbf{e}}) \in \mathcal{C}$ in (4). Since $\gamma_1 = k_1 + \alpha$ and $\gamma_2 = k_1\alpha$, the theorem will be proven by demonstrating that there exist $p^* > 0$, and, for any given $k_1 > 0$, there exists $\alpha^{**} > 0$, such that, for any $p \ge p^*$ and $\alpha \ge \alpha^{**}$, then $\lim_{t\to\infty} \tilde{e}_2 = 0$ holds. Then the result will follow by setting $\gamma_1^* = k_1 + \alpha^{**}$ and $\gamma_2^* = k_1\alpha^{**}$. To proceed, it is firstly recalled that global boundedness of the trajectories of system (4)–(5) (hence of $\dot{e}_2(t)$), has already been established in Properties 4.1 and 4.2. Then, consider system (7) (whose trajectories have been proven globally bounded within the Proof of Property 4.2), and regard the forcing term $\dot{e}_2(t)$ as a bounded exogenous disturbance. By selecting the Lyapunov function candidate $\mathcal{V} = \frac{1}{2}\tilde{e}_1^2 + \frac{1}{2}r_1^2$, it follows that the derivative of $\mathcal{V}$ around the trajectories of (7) satisfies (after an application of Young's inequality): $\dot{\mathcal{V}} \le -\frac{\alpha}{2}\tilde{e}_1^2 - \frac{k_1}{2}r^2 + r\left(\dot{e}_2 - \frac{\tilde{e}_1 p^2}{|\tilde{e}_1|p+\delta(t)}\right) - \frac{\alpha}{2}\tilde{e}_1^2 - \frac{k_1}{2}r^2 + \frac{\bar{\delta}}{2}r^2 + \frac{1}{2\bar{\delta}}\tilde{e}_1^2$, where $\bar{\delta} > 0$. It is then seen that, for any fixed $k_1 > 0$, it suffices to choose $\bar{\delta} \le k_1$ and, in turn, $\alpha \ge \frac{1}{\bar{\delta}}$ to obtain $-\frac{\alpha}{2}\tilde{e}_1^2 - \frac{k_1}{2}r^2 + \frac{\bar{\delta}}{2}r^2 + \frac{1}{2\bar{\delta}}\tilde{e}_1^2 \le 0$. Hence, once having fixed k_1, $\bar{\delta}$ and, in turn, α as described so as to fulfill the previous inequality, it follows: $\dot{\mathcal{V}} \le -\frac{\alpha}{2}\tilde{e}_1^2 - \frac{k_1}{2}r^2 + r\left(\dot{e}_2 - \frac{\tilde{e}_1 p^2}{|\tilde{e}_1|p+\delta(t)}\right)$. By integrating both sides of the previous inequality, one obtains $\mathcal{V}(t) + \int_0^t \frac{\alpha}{2}\tilde{e}_1^2 + \frac{k_1}{2}r^2 d\tau \le \mathcal{V}(0) + \int_0^t r\left(\dot{e}_2 - \frac{\tilde{e}_1 p^2}{|\tilde{e}_1|p+\delta(\tau)}\right)d\tau$. From Lemma 3, it is seen that there exist $p^* > 0$ and $\alpha^* > 0$ such that (9) holds. Hence, by defining $\alpha^{**} = \max\{\frac{1}{\bar{\delta}}, \alpha^*\}$, by selecting p and α such that $p \ge p^*$ and $\alpha \ge \alpha^{**}$, since $\mathcal{V}(t) \ge 0$, by using (9), one obtains: $\int_0^t \frac{\alpha}{2}\tilde{e}_1^2 + \frac{k_1}{2}r^2 d\tau \le \mathcal{V}(0) + J_\infty$. From the right-hand side of the previous inequality it follows that $\tilde{e}_1 \in \mathcal{L}_2$ (and that $r \in \mathcal{L}_2$); this, from Theorem 2, shows that $\lim_{t\to\infty} \tilde{e}_1 = 0$. This implies that $\int_0^t \dot{\tilde{e}}_1(\tau)d\tau$ has a finite limit as t converges to infinity, hence, by using Theorem 1, it can be established that $\lim_{t\to\infty} \dot{\tilde{e}}_1 = 0$. The proven convergence to zero of both $\tilde{e}_1$ and $\dot{\tilde{e}}_1$, along with the first equation in (6), finally implies that $\lim_{t\to\infty} \tilde{e}_2 = 0$. Hence $\hat{e}_2$ asymptotically learns e_2. □

5. Control system design

In preparation for control design, system (4) is conveniently re-arranged in state–space form as

$$\dot{\mathbf{e}} = A\mathbf{e} + B(u + \zeta(t)) \tag{10}$$

where the values of the matrices A and B are uniquely determined from (4). By defining then

$$P = \begin{pmatrix} \alpha_1 & \alpha_3 \\ \alpha_3 & \alpha_2 \end{pmatrix}, \quad Q = \begin{pmatrix} -\beta_1 & 0 \\ 0 & -\beta_2 \end{pmatrix} \tag{11}$$

the following Lyapunov equation is considered

$$PA + A^T P = -Q. \tag{12}$$

Next, the task is to show how to choose α_1, α_2 and α_3 in P such that Eq. (12) be fulfilled while guaranteeing, at the same time, that both matrices P and Q be positive-definite. To hence proceed, fix arbitrarily the compact sets in Assumption 3.1. Then, observe that Eq. (12), by virtue of (11) and (4), translates into the following set of *three* independent equations

$$\begin{aligned} -2\alpha_3 k &= -\beta_1 \\ \alpha_1 &= \alpha_2 k + \alpha_3 d \\ 2(\alpha_3 - \alpha_2 d) &= -\beta_2. \end{aligned} \tag{13}$$

From the first equation in (13), one obtains $\alpha_3 = \frac{\beta_1}{2k}$, which implies that for any chosen $\alpha_3 > 0$, the resulting β_1 in Q in (11) is always positive, since k is positive. As for β_2 in Q, from the third equation in (13) it follows that $\alpha_2 2d - 2\alpha_3 = \beta_2$, which implies that, once $\alpha_3 > 0$ has been fixed, since $d \in [d_m, d_M]$, with

$d_m > 0$, it is possible to choose $\alpha_2 > 0$ large enough such that $\beta_2 > 0$ in Q in (11); in particular, α_2 must fulfill $\alpha_2 > \frac{\alpha_3}{d}$. Next, a sufficient condition for having P in (11) positive-definite is that its leading minors be positive, that is: $\alpha_1 > 0$ and $\alpha_1\alpha_2 - \alpha_3^2 > 0$. A way to fulfill the first condition is yielded by the second equation in (13) which implies that α_1 is positive, since α_3 and α_2 have been chosen positive, and since k and d are both positive. As for the second condition, by replacing α_1 within it with the term on the right-hand side of (13), one obtains $\alpha_2^2 k + \alpha_3\alpha_2 d - \alpha_3^2 > 0$, which is implied by $\alpha_3\alpha_2 d - \alpha_3^2 > 0$, which is in turn fulfilled whenever $\alpha_2 > \frac{\alpha_3}{d}$. This is summarized in the following property.

Property 5.1. *For any given $[k_m, k_M]$, $[d_m, d_M]$ and $[b_m, b_M]$ in Assumption 3.1, it is always possible to choose $\alpha_3 > 0$, and, consequently, $\alpha_2 > 0$ large enough to fulfill $\alpha_2 > \frac{\alpha_3}{d}$, so that the Lyapunov equation (12) be satisfied, while having P and Q in (11) positive definite.*

Inspired by Wang et al. (2013, eq. (21)), the following two definitions will be used to characterize the control action u in (4):

Definition 5.1. The class $\mathcal{C}$ is the set of controllers:

$$u^*(t, \mathbf{e}, \hat{\mathbf{e}}) = -\frac{(\bar{\alpha}_3 e_1 + \bar{\alpha}_2 \hat{e}_2)\bar{\zeta}_\infty^2}{\left|\bar{\alpha}_3 e_1 + \bar{\alpha}_2 \hat{e}_2\right| \bar{\zeta}_\infty + \eta} \tag{14}$$

such that the constants $\bar{\alpha}_2, \bar{\alpha}_3, \bar{\zeta}_\infty$ and η are all positive.

Definition 5.2. Consider prescribed compact sets in Assumption 3.1. Then, define the class $\mathcal{C}_2 \subset \mathcal{C}$ as the set of controllers belonging to $\mathcal{C}$, such that:

(1) $\bar{\alpha}_2 = \alpha_2$ and $\bar{\alpha}_3 = \alpha_3$ in (14), where α_2 and α_3 are elements of the matrix P in (11) and are selected as a function of the compact sets in Assumption 3.1, as dictated by Property 5.1
(2) $\bar{\zeta}_\infty = \zeta_\infty$ in (14), where ζ_∞ satisfies $\zeta_\infty > |\zeta(t)|$.

The class $\mathcal{C}_2$ can hence be defined as the set of controllers:

$$u^{**}(t, \mathbf{e}, \hat{\mathbf{e}}) = -\frac{(\alpha_3 e_1 + \alpha_2 \hat{e}_2)\zeta_\infty^2}{\left|\alpha_3 e_1 + \alpha_2 \hat{e}_2\right| \zeta_\infty + \eta} \tag{15}$$

where the positive constants α_2, α_3 and ζ_∞ satisfy points (1) and (2) above, and where η is a positive constant.

The following theorem establishes the convergence properties of the regulation error $\mathbf{e}$ whenever $u \in \mathcal{C}_2$:

Theorem 5 (*Regulation-error Convergence*)**.** *For any given compact set $\mathcal{K} \subset \mathbb{R}^2$, any given set in Assumption 3.1, any given $\zeta(t)$ in (4), and for any desired $\epsilon > 0$, it is possible to choose a controller $u^{**}(t, \mathbf{e}, \hat{\mathbf{e}})$ in (15) with $\eta > 0$ small enough, and a learning observer in (5) with $p > 0$, $\gamma_1 > 0$ and $\gamma_2 > 0$ large enough, so that there exists $t^* > 0$, such that the regulation error $\mathbf{e}$ within the closed-loop trajectories (5)–(10) satisfies $\|\mathbf{e}\| \leq \epsilon$, for any initial condition $\mathbf{e}(0) \in \mathcal{K}$ and $\hat{\mathbf{e}}(0) \in \mathbb{R}^2$, and for any $t \geq t^*$.*

Proof. Fix arbitrarily: the compact set $\mathcal{K} \subset \mathbb{R}^2$, the sets in Assumption 3.1, and $\zeta(t) \in \mathcal{L}_\infty$ in (4). Then, consider the closed-loop system (5)–(10) satisfying $\mathbf{e}(0) \in \mathcal{K}$, $\hat{\mathbf{e}}(0) \in \mathbb{R}^2$, with $u = u^{**}(t, \mathbf{e}, \hat{\mathbf{e}}) \in \mathcal{C}_2$ in (10). Because $u^{**}(t, \mathbf{e}, \hat{\mathbf{e}}) \in \mathcal{C}_2 \subset \mathcal{C}$, then Properties 4.1 and 4.2 hold, and hence the closed-loop trajectories are well-defined for any $t \geq 0$ and uniformly bounded. Hence it is possible to regard the interconnection (5)–(10), as the sole system (10) forced by time-varying, uniformly bounded signals $u = u^{**}(t, \mathbf{e}, \hat{\mathbf{e}})$ and $\zeta(t)$. Consider then the Lyapunov function-candidate $\mathcal{W} = \mathbf{e}^T P \mathbf{e}$, where the matrix P is defined in Eq. (11) and the parameters α_2 and α_3 within it are chosen as dictated by Property 5.1: in this way, matrices P and Q in Eq. (11) are positive-definite, the quadratic form $\mathbf{e}^T P \mathbf{e}$ is positive-definite, and the Lyapunov equation (12) is satisfied. As a consequence, the derivative of $\mathcal{W}$ along the trajectories of system (10), with $u = u^{**}(t, \mathbf{e}, \hat{\mathbf{e}})$, can be shown to satisfy (after some algebra) $\dot{\mathcal{W}} \leq -\mathbf{e}^T Q \mathbf{e} + 2b\left(\frac{\zeta_\infty |\alpha_3 e_1 + \alpha_2 \hat{e}_2| \eta}{\zeta_\infty |\alpha_3 e_1 + \alpha_2 \hat{e}_2| + \eta}\right) + 2b\alpha_2 \tilde{e}_2 (u + \zeta(t))$. From the latter, by exploiting the existence (by construction) of a constant $\gamma > 0$ such that $-\mathbf{e}^T Q \mathbf{e} \leq -\gamma \mathcal{W}$, and by using $\frac{\zeta_\infty |\alpha_3 e_1 + \alpha_2 \hat{e}_2| \eta}{\zeta_\infty |\alpha_3 e_1 + \alpha_2 \hat{e}_2| + \eta} \leq \eta$, one can finally derive

$$\dot{\mathcal{W}} \leq -\gamma \mathcal{W} + 2b\eta + 2b\alpha_2 \tilde{e}_2 (u + \zeta(t)). \tag{16}$$

By then appealing to Theorem 4, it follows that there exist $p^* > 0$, $\gamma_1^* > 0$ and $\gamma_2^* > 0$, such that, for any $p \geq p^*$, $\gamma_1 \geq \gamma_1^*$ and $\gamma_2 \geq \gamma_2^*$ within the observer dynamics in (5), the estimation error $\tilde{e}_2$ converges to zero. Hence, by indeed selecting p, γ_1 and γ_2 so that $p \geq p^*$, $\gamma_1 \geq \gamma_1^*$ and $\gamma_2 \geq \gamma_2^*$ in (5), then, the term $2b\alpha_2 \tilde{e}_2 (u + \zeta(t))$ in (16) converges to zero as well. Hence, by applying the Comparison Lemma (Khalil, 2002, p. 102) to inequality (16), it is seen that once $\epsilon > 0$ has been fixed, it is possible to choose $\eta > 0$ small enough in (15), hence in (16), such that there exists a time $t^* > 0$, such that for any $t \geq t^*$, then $\|\mathbf{e}\| \leq \epsilon$, as requested. □

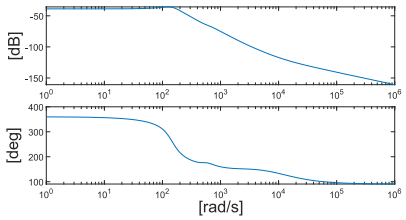

Fig. 2. Bode plot of identified plant (1)–(2).

6. Experimental results

The proposed control strategy is evaluated experimentally by driving the bottom loudspeaker with random noise, with the aim of emulating vibrations experienced in fabrication environments. The experimental investigation is additionally complemented by comparing the performance of the proposed algorithm to the one of a PID controller, under the same experimental conditions.

By setting the sampling frequency to 1 kHz, the PID controller is designed on the basis of a preliminary system-identification shown in Fig. 2. By using the "PID tuner" feature in Simulink, and by selecting the PID transfer function as $P(s) = k_p + k_i \frac{1}{s} + k_d \frac{s}{T_f s + 1}$, the desired closed-loop bandwidth is pushed to 100 Hz with the aim of enforcing a fast transient performance in terms of rise time, settling time and peak time, whereas the phase-margin is set to 64.5 degrees so as to dictate a good performance in terms of the percentage-overshoot indicator. The resulting PID controller gains are as follows: $k_p = 647$, $k_i = 3.35 \times 10^4$, $k_d = 3.08$, and $T_f = 1.39 \times 10^{-5}$. Whereas, the resulting overall closed-loop system performance reads as: rise time = 0.00217 s, settling time = 0.0363 s, overshoot = 10.7%, peak = 1.11, and gain margin = 30.8 dB at 2.68×10^4 rad/s.

The nonlinear control strategy is tuned by exploiting the results derived in the convergence analysis, aided by computer simulations. With reference to the control action defined in (15), in view of the inequality in (16), the gain η is selected by seeking a trade-off between the achievable tracking performance and the control system's physical capability of generating high-frequency commands. The parameters α_2 and α_3 are chosen in conformity with Property 5.1, whereas the gain ζ_∞, because of Definition 5.2, point (2), is selected to reflect an upper bound on the magnitude of the expected disturbance affecting the error system in (4). This

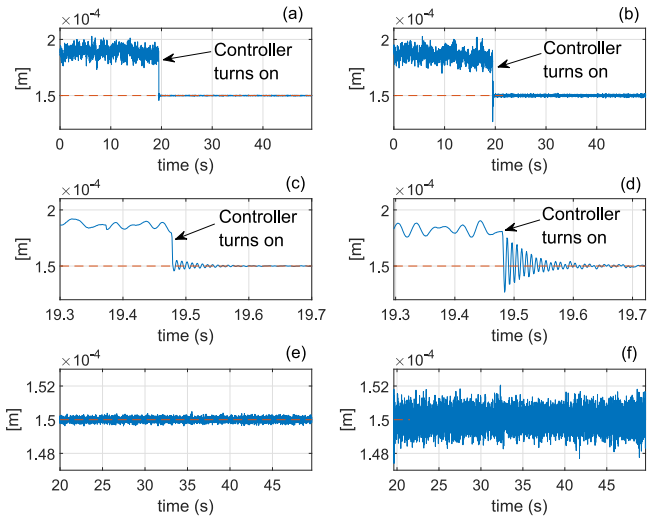

Fig. 3. Setpoint regulation comparative performance: actual distance $x_1(t)-\xi(t)$ vs desired distance $c = 1.5 \times 10^{-4}$. Plots on the left for the proposed strategy, plots on the right for the PID strategy. Plots (a) and (b) feature the entire time history; plots (c) and (d) zoom on the transition from control off to control on; plots (e) and (f) display the steady-state.

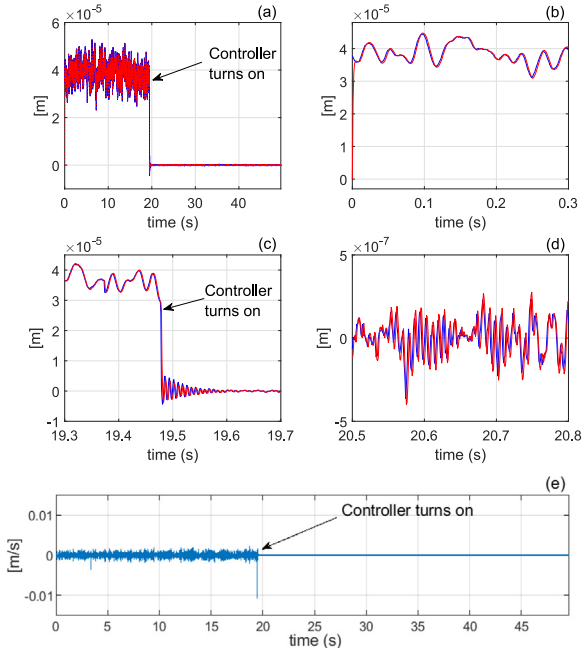

Fig. 4. Observer performance: tracking (e_1 vs. $\hat{e}_1$) over the entire experiment (a); zoomed tracking during the initial transient (b); zoomed tracking on the transition from control off to control on (c); zoomed tracking during (part of) the steady-state (d); estimated regulation-error velocity $\hat{e}_2$ (e).

results in: $\eta = 10$, $\alpha_2 = 0.8$, $\alpha_3 = 100$, and $\zeta_\infty = 10$. The tuning of the control system is completed by fixing $k_1 = 1$ within the preliminary control action defined in Section 3. The observer parameters γ_1, γ_2 and p in (5) are selected in conformity with Theorem 4, whereas the function $\delta(t)$ is chosen as a decaying exponential so that $\int_0^t \delta(\tau)d\tau$ be a uniformly bounded function of time, as required by Definition 4.1. The resulting observer parameters are: $\gamma_1 = 1000$, $\gamma_2 = 20$, $p = 4 \times 10^4$, and $\delta(t) = e^{-t}$.

For both strategies, the desired distance is set to $c = 1.5 \times 10^{-4}$ m, while driving the sample with random noise. The experiments are carried out by initially keeping the control signal inactive, so as to highlight the effect of the uncompensated vibrations on the time evolution of the distance between the metrology platform and the sample (see Fig. 3). Upon turning the control system on, Fig. 3 shows that both strategies are capable to steer the systems' trajectories towards an attractor within which the regulation error e_1 is substantially reduced. Moreover, both strategies display a similar settling time towards their respective attractor. However, from Fig. 3 it is seen that the proposed strategy exhibits a lesser overshoot along with a more favorable steady-state in which the set-point regulation is indeed carried out with superior accuracy as compared to the PID strategy. The performance of the learning observer is synthetically displayed in Fig. 4, from which it can be seen that the observer is capable to effectively reconstruct the measured distance, whose information is in turn used to produce the estimated regulation-error velocity $\hat{e}_2$ (Fig. 4(e)).

7. Conclusions

In this work, a nonlinear control strategy is presented for locking the distance between a metrology platform and a sample within a laboratory prototype. The sample is driven with random noise with the aim of recreating environmental vibrations in fabrication environments. The proposed control strategy relies on a novel observer capable of reconstructing the missing velocity-information, in spite of unknown system parameters. Robust stability is then secured by a combination of high-gain and high-frequency tools. A comparative experimental study with a PID-based control-strategy shows that the proposed algorithm is effective in achieving the control task, and that it is capable to do so, overall, in a more effective way than its PID-based counterpart. Future investigations will consider the extension of the present design to a six-degree of freedom problem.

Appendix

A.1. Proof of Property 4.1

Proof. The proof of points (1), (2) and (3) follows by noticing that, by virtue of inequalities $\frac{|e_1-\hat{e}_1|p^2}{|e_1-\hat{e}_1|p+\delta(t)} \leq p$, and $\left|\frac{(\bar{\alpha}_3 e_1+\bar{\alpha}_2\hat{e}_2)\bar{\zeta}_\infty^2}{|\bar{\alpha}_3 e_1+\bar{\alpha}_2\hat{e}_2|\bar{\zeta}_\infty+\eta}\right| \leq \bar{\zeta}_\infty$, system (5)–(10), with $u = u^*(t, \mathbf{e}, \hat{\mathbf{e}}) \in \mathcal{C}$, can be regarded as a linear system forced by perturbations which are uniformly bounded, continuous in t and locally Lipschitz in the state $(\hat{\mathbf{e}}, \mathbf{e})^T$. □

A.2. Proof of Property 4.3

Proof. Fix arbitrarily: the compact set $\mathcal{K} \subset \mathbb{R}^2$, the sets in Assumption 3.1, and $\zeta(t) \in \mathcal{L}_\infty$ in (4). Then, consider system (5)–(10), with $\mathbf{e}(0) \in \mathcal{K}$, $\hat{\mathbf{e}}(0) \in \mathbb{R}^2$ and $u = u^*(t, \mathbf{e}, \hat{\mathbf{e}}) \in \mathcal{C}$ in (10). Choose arbitrarily $\epsilon > 0$; then Property 4.1 shows that there exists $p^* > 0$ such that

$$|\dot{e}_2| + \epsilon \leq p \quad \text{for } p \geq p^*, \ t \geq 0. \tag{A.1}$$

In view of (A.1), inequality (8) will be demonstrated by showing that there exist $\alpha^* > 0$, and $t_1 > 0$ such that:

$$\frac{1}{\alpha}|\ddot{e}_2| < \epsilon \quad \text{for } \alpha \geq \alpha^*, \ t \geq t_1. \tag{A.2}$$

With this aim, define $z \triangleq \bar{\alpha}_3 e_1 + \bar{\alpha}_2 \hat{e}_2$, and $f(z) \triangleq \frac{z\zeta_\infty^2}{|z|\zeta_\infty+\eta}$. From system (10), it follows that $\frac{1}{\alpha}\ddot{e}_2 = \frac{1}{\alpha}\left(-k\dot{e}_1 - d\dot{e}_2 + b\left(-\frac{\partial f}{\partial z}\frac{\partial z}{\partial t} + \frac{\dot{\zeta}(t)}{b}\right)\right)$, whereas Property 4.1, point (3), implies the existence

of $\bar{\alpha}_1 > 0$ such that: $\frac{1}{\alpha}\left(|k\dot{e}_1| + |d\dot{e}_2| + |\dot{\zeta}(t)|\right) < \frac{\epsilon}{2}$ for $\alpha \geq \bar{\alpha}_1$. Hence, by finding $\alpha^* \geq \bar{\alpha}_1$ and $t_1 > 0$ such that

$$\frac{1}{\alpha} b \left| \frac{\partial f}{\partial z} \frac{\partial z}{\partial t} \right| < \frac{\epsilon}{2} \quad \text{for } \alpha \geq \alpha^*,\ t \geq t_1 \tag{A.3}$$

then inequality (A.2) will follow. To this end, by considering that $\frac{\partial f(z)}{\partial z} = \frac{\zeta_\infty^2 \eta}{(|z|\zeta_\infty + \eta)^2} \leq \frac{\zeta_\infty^2}{\eta}$, since $\frac{1}{\alpha}\frac{\partial z}{\partial t} = \frac{1}{\alpha}(\alpha_3 \dot{e}_1 + \alpha_2 \dot{\hat{e}}_2)$, it is seen that (A.3) is implied by:

$$b \frac{\zeta_\infty^2}{\eta} \frac{1}{\alpha} \left| \alpha_3 \dot{e}_1 + \alpha_2 \dot{\hat{e}}_2 \right| < \frac{\epsilon}{2} \quad \text{for } \alpha \geq \alpha^*,\ t \geq t_1. \tag{A.4}$$

Because of Property 4.1, there exists $\bar{\alpha}_2 \geq \bar{\alpha}_1$ such that $b\frac{1}{\alpha}\frac{\zeta_\infty^2}{\eta}$ $|\alpha_3 \dot{e}_1| < \frac{\bar{\beta}_2}{\alpha} < \frac{\epsilon}{4}$ holds for $\alpha \geq \bar{\alpha}_2$. This implies that for proving (A.4) it is sufficient to show that there exist $\bar{\alpha}_3 \geq \bar{\alpha}_2$ and $t_1 \geq 0$, such that $b\frac{1}{\alpha}\frac{\zeta_\infty^2}{\eta}\left|\alpha_2 \dot{\hat{e}}_2\right| < \frac{\epsilon}{4}$ holds for $\alpha \geq \bar{\alpha}_3$ and $t \geq t_1$. Furthermore, by virtue of the identity $\frac{1}{\alpha}\dot{\hat{e}}_2 = k_1 \tilde{e}_1 + \frac{1}{\alpha}\frac{\tilde{e}_1 p^2}{|\tilde{e}_1| p + \delta(t)}$, the previous inequality translates into $b\frac{\zeta_\infty^2}{\eta}\alpha_2 \left| k_1 \tilde{e}_1 + \frac{1}{\alpha}\frac{\tilde{e}_1 p^2}{|\tilde{e}_1| p + \delta(t)} \right| < \frac{\epsilon}{4}$ for $\alpha \geq \bar{\alpha}_3,\ t \geq t_1$, which is in turn implied by:

$$b \frac{\zeta_\infty^2}{\eta} \alpha_2 \left| \frac{1}{\alpha} \frac{\tilde{e}_1 p^2}{|\tilde{e}_1| p + \delta(t)} \right| < \frac{\epsilon}{8} \quad \text{for } \alpha \geq \bar{\alpha}_3,\ t \geq t_1$$

$$b \frac{\zeta_\infty^2}{\eta} \alpha_2 \left| k_1 \tilde{e}_1 \right| < \frac{\epsilon}{8} \quad \text{for } \alpha \geq \bar{\alpha}_3,\ t \geq t_1. \tag{A.5}$$

The final task is hence to prove the inequalities in (A.5). To this end, Property 4.1 shows that $\frac{\tilde{e}_1 p^2}{|\tilde{e}_1| p + \delta(t)} + \dot{e}_2 \in \mathcal{L}_\infty$, hence, the steady state evolution of $r(t)$ in (7) must possess an upper bound which is dictated by p, $\dot{e}_2$ and k_1, but not by $\tilde{e}_1$. As a result, once k_1 and p have been fixed, for any $\bar{\epsilon} > 0$ it is possible to choose $\bar{\alpha}(\bar{\epsilon}) > 0$ large enough such that there exists $\bar{t}_1 > 0$, such that for any $\alpha \geq \bar{\alpha}(\bar{\epsilon})$ and for any $t \geq \bar{t}_1$, then $|\tilde{e}_1| < \bar{\epsilon}$. This implies that there exists $\bar{\alpha}_3 > 0$ and, in turn, $t_1 \geq 0$ such that the second inequality in (A.5) holds. In addition, inequality $\frac{|\tilde{e}_1| p^2}{|\tilde{e}_1| p + \delta(t)} \leq p$ implies the existence of $\underline{\alpha}_4 > 0$ such that $b\frac{\zeta_\infty^2}{\eta}\alpha_2 \left| \frac{1}{\alpha}\frac{\tilde{e}_1 p^2}{|\tilde{e}_1| p + \delta(t)} \right| < \frac{\epsilon}{8}$ for $\alpha \geq \underline{\alpha}_4$ and $t \geq 0$. Hence, by choosing $\bar{\alpha}_3 > \underline{\alpha}_4$, the first inequality in (A.5) is fulfilled, too. Fixing $\alpha^* = \bar{\alpha}_3$, concludes the proof. □

References

Eaton, P., & West, P. (2010). *Atomic force microscopy*. Oxford University Press.

Egeland, O., & Gravdahl, J. T. (2003). *Modeling and simulation for automatic control*. Marine Cybernetics.

Esfandiari, F., & Khalil, H. K. (1992). Output feedback stabilization of fully linearizable systems. *Internat. J. Control*, *56*(5), 1007–1037.

Ito, S., Neyer, D., Pirker, S., Steininger, J., & Schitter, G. (2015). Atomic force microscopy using voice coil actuators for vibration isolation. In *2015 IEEE international conference on advanced intelligent mechatronics (AIM)*.

Khalil, H. K. (2002). *Nonlinear systems*. Prentice-Hall.

Leach, R. (2009). *Fundamental principles of engineering nanometrology*. Elsevier.

Subrahmanyan, P. K. (1999). *A model approach to precision motion control* (PhD thesis), MIT.

Thier, M., Saathof, R., Sinn, A., Hainisch, R., & Schitter, G. (2016). Six degree of freedom vibration isolation platform for in-line nano-metrology. In *Proceedings of the 7th IFAC symposium on mechatronic systems*.

Wang, Y., Zhang, Z., Li, L., & Lu, J. (2013). Simple adaptive asymptotic tracking scheme for parametric strict-feedback nonlinear systems with additive disturbance. *Math. Probl. Eng.*.

Xian, B., Dawson, D., de Queiroz, M., & Chen, J. (2004). A continuous asymptotic tracking control strategy for uncertain nonlinear systems. *IEEE Trans. Automat. Control*, *49*(7), 1206–1211.

Saverio Messineo received the Ph.D. degree in Control Systems at the Norwegian University of Science and Technology (NTNU), Trondheim, Norway, in 2009. While pursuing his Ph.D. studies, he spent more than two years, from 2006 to 2008, as a visiting Ph.D. student at the Department of Electrical and Computer Engineering at The Ohio State University, Columbus, Ohio, under the scientific supervision of Prof. Andrea Serrani. During his research career, he has been engaged in the investigation of problems within the area of control systems, either within an industrial framework (e.g., as a research scientist at the Schlumberger Gould Research Centre, Cambridge, UK), or in academia, while holding the post of associate professor in control systems at NTNU. From a theoretical standpoint, his research interests lie in the field of adaptive and robust nonlinear control design, nonlinear observer design, quasi-periodic disturbance rejection and nonlinear output regulation. In relation to the applicative side, he has been working in the experimental investigation of areas such as offshore crane control for marine operations, control of directional drilling systems for petroleum engineering applications, control of atomic force microscopes, and active vibration rejection for metrology platforms within the context of precision control for mechatronics systems.